Aquatic Decomposition of Mammalian Corpses: A Forensic Proteomic Approach

Haruka Mizukami[1], Bella Hathway[1] and Noemi Procopio[1*]

[1] The Forensic Science Unit, Faculty of Health and Life Sciences, Ellison Building, Northumbria University, Newcastle Upon Tyne, UK

* Corresponding author
Email address for correspondence: noemi.procopio@northumbria.ac.uk

Abstract

Methods currently available to estimate the *post-mortem submerged interval* (PMSI) of cadavers in water suffer from poor accuracy, being mostly based on morphological examination of the remains. Proteins present within bones have recently attracted more attention from researchers interested in the estimation of the *post-mortem interval* (PMI) in terrestrial environments. Despite the great potential of proteomic methods for PMI estimation, their application to aquatic environments has not yet been explored. In this study, we examined whether four different types of aquatic environment affected the proteome of mice bones with increasing PMSIs. Results showed that increasing PMSIs can influence the protein abundances more than the different types of water. In particular, the abundance of the muscle protein fructose-bisphophate aldolase A constantly decreased with increasing PMSIs. Additionally, the protein peptidyl-prolyl cis-trans isomerase showed a significant decrease between controls and aquatic environments. Furthermore, coagulation factor VII was deamidated only in submerged samples and not in terrestrial controls. Finally, fetuin-A was significantly more deamidated in pond water compared to the other aquatic environments. Overall, this study identified novel potential biomarker candidates that would be useful for the estimation of the PMSI and for the characterization of the type of water involved in criminal investigations.

Keywords: Bone proteomics, Forensic proteomics, Post-mortem submerged interval, LC-MS/MS, Aquatic decomposition, Forensic taphonomy, Forensic science, Post-translational modification, Skeletal remains, Biological aging

Introduction

The estimation of the time since death (or *post-mortem interval,* PMI) is useful in providing forensic information that can contribute to criminal investigation, in helping to identify the post mortem remains and/or a suspect, by narrowing down the range of time to be considered[1, 2] and helping to predict the condition of a body after a specific PMI. Forensic pathologists can estimate PMI on the bases of body alterations including the observation of rigor mortis[3], the measurement of body temperature[4], the succession of insects on the remains[5] or the usage of accumulated degree days (ADD)[6, 7]. However, PMI estimation is one of the most challenging themes in forensic science due to the high number of exogenous and endogenous factors that can affect the rate of decomposition, such as the type of soil surrounding a cadaver, temperature, and the presence of scavengers and insects[8, 9]. Furthermore, some of the methods previously mentioned cannot be applied to advanced stages of decomposition and yield inaccurate results when estimates of the time since death are attempted[1, 10].

When dealing with bodies found in aquatic environments, the estimation of the *post-mortem submerged interval* (PMSI) is even more complex and less well understood than PMI estimation in terrestrial cadavers. In fact, a large number of environmental variables, such as salinity, tides and water depth, temperature, and bacterial and chemical composition of the water[11-13] can complicate investigations and lead to erroneous estimations. One of the most classical approaches to the estimation of the PMSI involved the use of the aquatic decomposition score (ADS)[11, 14, 15], which measures the degree of decomposition of several areas of the body (face and neck, body and limbs) of recovered remains found in water. The ADS method has been used to develop models to predict the PMSI of bodies recovered in salt[15] and in fresh water[16], however several limits on the use of this approach have been raised so far[17]. Other studies have investigated the potential of accumulated degree days (ADD), normally used in terrestrial environments to estimate PMI, as means to estimate PMSI in fresh[14] and saltwater[16]. Despite the promising correlation found between ADS, AAD and PMSI, more research is required to overcome the subjectivity of these approaches. In fact, although these methods could be used to predict PMIs in cases of aquatic decomposition, the modifications are provisional and the assessments highly examiner-dependent[12]. Moreover, the action of both aquatic scavengers and water flow can result in the abrasion of the body

and in the acceleration of the skeletonization process. As a consequence, some parts of a body may be lost[12, 18], preventing the correct application of the ADS model. Other methods evaluated in the past include the assessment of adipocere formation[19, 20], and the evaluation of marine bacteria, insect, and algal successions[13, 21, 22]. The parameters studied were found to be strongly affected by the temperature[23, 24] and type of water[14], and by seasonality[25].

More recently, molecular-based approaches involving the analysis of proteins[26-31] and RNA[32, 33], have been adopted to better characterize the decomposition of the bodies. In particular, with the latest advances in mass spectrometry (MS) instrumentation and technology, proteomics has been increasingly used in the investigation of potential biomarkers correlated with the PMI.

Kwak *et al.*[27] used two-dimensional sodium dodecyl sulphate – polyacrylamide gel electrophoresis (SDS-PAGE) and high-performance liquid chromatography coupled with tandem mass spectrometry (HPLC-MS/MS) to analyze protein samples extracted from either the liver or heart of decomposing rats and found that 14 and 12 proteins, respectively, were modified according to the PMI (0,24 and 48 hours after death). Choi *et al.*[31] also conducted SDS-PAGE and LC-MS/MS analyses on proteins recovered from the skeletal muscle of rat and mouse, and found two proteins (eEF1A2 and GAPDH) that showed constant degradation patterns with the increase of PMI (0, 24, 28, 72 and 96 hours after death). These two studies confirmed that proteins in soft tissues were degraded or altered in a time-dependent manner. However, proteomic analyses on soft tissues, including brains, muscles and organs, can be affected by several environmental factors, such as temperature and heat[29, 30, 34] and are not applicable to more advanced decomposition stages.

In order to overcome the previously mentioned limitations, bones can be used as a target for biomolecular studies on PMI, being one of the tissues that survives the longest post mortem, being quite stable against extrinsic factors[18, 35]. Bones have been widely studied with particular focus on their inner/molecular composition (e.g., DNA degradation[36], the presence of radio-active isotope[37], microarray analysis[38] and microscopic imaging[39, 40]) and on their morphological aspects (e.g., the degree of bone weathering[41]). Proteins, in particular, can survive within the bone structure for prolonged periods after death[42, 43].

Bones are made up of an inorganic phase (50-70%) that contains mainly calcium phosphate (hydroxyapatite; HA) and by an organic phase (20-40%) that contains mainly proteins[35, 44]. Within the organic phase, there are two types of proteins; collagenous proteins (85-90%) and

non-collagenous proteins (NCPs)(10-15%)[44]. NCPs are tightly attached to the mineral matrix of the bone, and for this reason are particularly stable[45] and well preserved in archaeological and fossil samples[46-48] of different geochronological age. Thus, they are also good candidates for forensic studies, where it is essential to identify molecular candidates that are readily preserved, extracted and identified at each decomposition stage, at various times after death and in different environmental conditions to which the body has been subject.

The earliest attempt to seek associations between the degradation of bone proteins and PMI was made by Boaks *et al.*[49] using Sirius Red/Fast Green collagen staining, where collagenous proteins are stained red and NCPs are stained green. They collected bone samples from pigs deposited on the ground surface at zero-, two-, four-, six-, ten- and twelve-months post mortem and observed that the ratio of collagen proteins to NCPs significantly decreased at 10 months. Later, Jellinghaus *et al.*[50] conducted a similar study and suggested that bone protein degradation could be used as means to estimate PMI. More recently, Procopio *et al.*[51] performed LC-MS/MS analysis on bone samples of buried pigs allowed to decompose for time interval ranging from one month to one year post mortem to evaluate linkages between protein survival and PMI, i.e., the amount and variety of proteins after several PMIs. They found that the complexity of the proteome significantly decreased from 66 proteins found after 6 months to 19 found after one year post mortem, thus confirming that proteins present within bones can show time-related degradation patterns as previously shown by Kwak *et al.*[27] and Choi *et al*.[31] in soft tissues and organs. Procopio *et al.*[51] also targeted a specific protein (fetuin-A) previously found to be a useful biomarker for chronological age estimation[52] and showed that its abundance was consistent in individuals of similar age, regardless of their PMI. They also found that the deamidation ratios of biglycan at each PMI (one-, two-, four- and six-months) significantly increased with increasing PMIs in a time-dependent manner[51]. Recently, Prieto-Bonete *et al.*[45] used a similar approach to identify a human proteomic profile able to distinguish bones in which the PMI was either five or twenty years. In addition to the use of proteomic methods for the analysis of bone samples, similar proteomics methodologies have been already successfully applied to distinct fields of forensics, for example to map specific blood signatures from fingerprints[53] and to evaluate the fingermark ageing[54], further demonstrating their strength and suitability for various forensic applications.

Overall, all the studies[45, 49-52] mentioned above demonstrated the feasibility of the application of proteomic studies to forensic sciences, and in particular, to the estimation of the PMI. However, this approach has not so far been applied in water decomposition experiments and, for this reason, its applicability in aquatic environments remains unknown.

In this study, we investigated the effects of two variables on aquatic decomposition and the resulting bone proteomes of animal models; these were (1) the type of water (tap as control, pond water, saltwater and chlorinated water) and (2) the PMSI (e.g., zero-, one- and three-weeks). All the other environmental variables, such as temperature and water depth, were kept fixed to limit the complexity of the experiment and interpretation of the results. Proteins extracted from bones were quantified using a label-free methodology, and deamidation ratios of each protein were evaluated to look for potential biomarkers for PMSI estimation and for the interpretation of the deposition environment (e.g., terrestrial vs aquatic, type of water, and potential for movements of the body from one environment to another).

Experimental section

Materials and sample preparation

A total of 22 mouse carcasses (*Mus Musculus*) were purchased frozen from an U.K. supplier (operating in compliance with the Animal Welfare Act 2006). Ethical approval from Northumbria University was obtained for this experiment, with the submission reference 12125. 16 mice were soaked individually in bottles containing four types of water: tap water, saltwater, pond water and chlorinated water. The saltwater was collected from the North Sea (Tynemouth, U.K.), the chlorinated water was collected from a local swimming pool (Newcastle, U.K.) and the pond water from a local pond (Newcastle, U.K.). The tap water samples (labelled FM in the Results) were used as controls. Water collection was performed in October 2018. The tail of each mouse was taped to the bottom of the bottle in order to maintain the mouse at the same depth. All bottles were closed with their lids and placed under a fume cupboard for the whole duration of the experiment. For each type of water and PMSI tested, two identical mice were used as replicates and subjected to the same experimental treatment. The mice were then retrieved from each bottle at the selected PMSI

(one- or three-weeks) and tibiae (as indicated by Procopio *et al.*[52]) were collected from each individual straight after their recovery from the water. Additionally, two mice out of the 22 were allowed to defrost and tibiae were collected straight after (time zero control samples) without immersion in water (see Table 1). Terrestrial controls – four mice out of 22 left to decompose in a clear foil box in the same laboratory conditions (temperature 20°C, no access to insects or scavengers) for one- and three-weeks – were also included.

As a result, 44 bone samples of tibiae (both left and right) were retrieved. For the experiment, only the left tibiae were used, reducing the number of samples subjected to protein extraction and LC-MS/MS back to 22.

For the whole duration of the experiment the room temperature was kept at 20 °C and the water temperature was assumed to be constant at this temperature. The water pH for each bottle was measured at time zero and then every week, from week one to week three.

Table 1. List of samples used in the study with sample IDs and codes

Sample ID	Type of water	PMSI (weeks)	Biological replicates (codes)
FM1	Tap water	1	FM1_1, FM1_2
FM3		3	FM3_1, FM3_2
SM1	Saltwater	1	SM1_1, SM1_2
SM3		3	SM3_1, SM3_2
PM1	Pond water	1	PM1_1, PM1_2
PM3		3	PM3_1, PM3_2
CM1	Chlorinated water	1	CM1_1, CM1_2
CM3		3	CM3_1, CM3_2
CTRL	Not submerged in water	0	CTRL1, CTRL2
FB1	Foil box (not submerged)	1 (PMI)	FB1_1, FB1_2
FB3		3 (PMI)	FB3_1, FB3_2

Protein extraction

Formic acid (FA), hydrochloric acid (HCl), sodium hydroxide (NaOH) were purchased from Fisher Scientific (U.K.). Guanidine hydrochloride (GuHCl) and iodoacetamide (IAM) were purchased from Sigma-Aldrich (U.K.). Tris and acetonitrile (ACN) were obtained from Thermo Fisher Scientific (U.K.). Dithiothreitol (DTT) and trifluoroacetic acid (TFA) were purchased from Fluorochem (U.K.) and Alfa Aesar (U.K.), respectively. Ammonium acetate (AA) was purchased from Scientific Laboratory Supplies (U.K.). Sequencing grade modified trypsin was purchased

from Promega (U.K.). Molecular weight cut-off (MWCO) ultrafiltration filter (Vivaspin®500 polyethersulfone, 10 kDa) was purchased from Sartorius (Germany). OMIX C18 pipette tips (10-100 µL) were purchased from Agilent Technologies (US).

Proteins were extracted following the protocol proposed by Procopio and Buckley[42]. Collected bones were cleaned in deionized water and dried in a fume cupboard at room temperature. Tibiae were broken in half; one half was treated for protein extraction and the other half was preserved at room temperature. Each sample was decalcified with 1 mL of 10 v/v% FA for 6 hours at 4 °C. After removing all the acid soluble fraction, the acid insoluble fraction was incubated for 18 hours at 4°C with 500 µL of 6 M GuHCl/100mM TRIS buffer (pH 7.4). The buffer was exchanged into 100 µL of 50 mM AA with 10K MWCO filters, and samples were then reduced with 4.2 µL of 5 mM DTT for 40 min at room temperature and alkylated with 16.8 µL of 15 mM IAM for 45 min in the dark at room temperature[55]. Samples were then quenched with another 4.2 µL of 5 mM DTT, then digested with 0.4 µg of trypsin for 5 hours at 37°C and finally frozen. By adding 15 µL of 1 v/v% TFA, the digestion was stopped and the samples were then desalted, concentrated and purified using OMIX C18 pipette tips with 0.1 v/v% TFA as washing solution and 50 v/v% ACN/0.1 v/v% TFA as a conditioning solution. In short, the pipette tips were prepared with two volumes of 100 µL of 0.1 v/v% TFA and washed twice with 100 µL of 50 v/v% ACN/0.1 v/v% TFA. The sample was then aspirated into the tip at least ten times to efficiently bind peptides to the absorbent membrane. Finally, two wash steps with 100µL of 0.1 v/v% TFA were performed, and then the peptides were eluted into 100 µL of 50 v/v% ACN/0.1 v/v% TFA. Purified peptides were left in the fume cupboard with lids open to dry them completely at room temperature prior to their submission for LC-MS/MS analysis.

LC-MS/MS analysis

Samples resuspended in 5 v/v% ACN/0.1 v/v% TFA were analyzed by LC-MS/MS using an Ultimate™ 3000 Rapid Separation LC (RSLC) nano LC system (Dionex Corporation, Sunnyvale, CA, USA) coupled to a Q Exactive™ Plus Hybrid Quadrupole-Orbitrap Mass Spectrometer (Thermo Fisher Scientific, Waltham, MA, USA). Peptides were separated on an EASY-Spray™ reverse phase LC Column (500 mm x 75 µm diameter (i.d.), 2 µm, Thermo Fisher Scientific, Waltham, MA, USA) using a gradient from 96 v/v% A (0.1 v/v% FA in 5 v/v% ACN) and 4 v/v%

B (0.1 v/v% FA in 95 v/v% ACN) to 8 v/v%, 30 v/v% and 50% B at 14, 50, and 60 min, respectively, at a flow rate of 300 nL min^{-1}. Acclaim™ PepMap™ 100 C18 LC Column (5 mm x 0.3 mm i.d., 5 µm, 100 Å, Thermo Fisher Scientific) was used as trap column at a flow rate of 25 µL min^{-1} kept at 45 °C. The LC separation was followed by a cleaning cycle with an additional 15 min of column equilibration time. Then, peptide ions were analyzed in full scan MS scanning mode at 35,000 MS resolution with an automatic gain control (AGC) of $1e^6$, injection time of 200 ms and scan range of 375-1,400 m/z. The top ten most abundant ions were selected for data-dependent MS/MS analysis with a normalized collision energy (NCE) level of 30 performed at 17,500 MS resolution with an AGC of $1e^5$ and maximum injection time of 100 ms. The isolation window was set to 2.0 m/z, with an underfilled ratio of 0.4%, dynamic exclusion was employed; thus, one repeat scan (i.e., two MS/MS scans in total) was acquired in a 45 s repeat duration with the precursor being excluded for the subsequent 45 s.

Protein identification and statistical analysis

Peptide mass spectra were then searched against the Swiss-Prot database using the Mascot search engine (version 2.5.1; www.matrixscience.com) for matches to primary protein sequences, specifying the taxonomy filter to *Mus musculus* (house mouse). This search included the fixed carbamidomethyl modification of cysteine as it results from addition of DTT to proteins. In the light of our aims, deamidation (asparagine and glutamine) and oxidation (lysine, methionine and proline) were also considered as variable modifications. The enzyme was set to trypsin with a maximum of two missed cleavages allowed. Mass tolerances for precursor and fragmented ions were set at 5 ppm and 0.5 Da, respectively. It was assumed that all spectra hold either 2+ or 3+ charged precursors.

Progenesis software (version 4.1; Nonlinear Dynamics, Newcastle, U.K.) was used to identify the proteins and assess their relative abundance in each sample. The relative abundance of the proteins present in the samples is calculated by the software by measuring the peptide ion abundances as a result of the sum of the areas under the curve for each peptide ion. The software normalizes each LC-MS/MS run against a reference run automatically selected as the normalization reference, to take into account and to correct systematic experimental variations that can occur between different runs. Then, it enables protein comparisons among different experimental conditions and the identification of protein expression changes. Peptide ions with a score of <27, which indicates identity or

extensive homology ($p < 0.05$), were excluded from the analysis based on the Mascot evaluation of the peptide score distribution. To further increase the reliability of the obtained results, proteins with a peptide count of <2 were also excluded from further analysis.

Principal Component Analysis (PCA) was performed on the normalized abundance values exported from Progenesis, using R software with the factoextra, pca3d, car and rgl packages, using proteins sorted by their ANOVA FDR adjusted *p* value (or "*q* value"), in order to exclude the ones that showed similar relative abundances across different conditions (and that did not contribute to cluster separations). The threshold used for each PCA were specified from time to time in the figures' captions.

In order to measure the deamidation ratios, only peptides that showed both non-deamidated and deamidated forms (i.e., peptides that have either deamidated asparagine (N) or deamidated glutamine (Q) and the non-deamidated form) were selected for further investigation (Step 1). For each of these peptides, the deamidation ratio was calculated using the following equation:

$$Deamidation\ ratio\ [\%] = \frac{Total\ relative\ abundance\ of\ deamidated\ states}{Total\ relative\ abundance\ of\ the\ peptide} \times 100$$

Student's t-Test *p* value was then used to evaluate the significance of the deamidation ratios comparing the two different conditions (Step 2). Only peptides whose Student's t-Test *p* value between two different conditions (i.e., between different types of water at the same PMSI or between different PMSIs in the same type of water) was smaller than 0.05 were selected for further analysis (Step 3).

Results and Discussion

Water pH change at different PMSI

The pH of the water was recorded for the whole duration of the experiment (Supporting Table S-1). After averaging the values for the two biological replicates and calculating standard error (SE) values (Fig. 1), we found similar trends in the variation of pH at specific PMSIs within all the water types tested. At time zero (e.g., prior to the immersion of the mouse in water), tap water was the most alkaline (pH 7.33), followed in decreasing pH by saltwater (pH 7.06), chlorinated water (pH 6.99) and pond water (pH 6.87). The pH drastically

decreased at one-week PMSI, where saltwater became the most acidic environment (average pH 5.75) and where the other three types of water showed a similar pH value (average pH 6.17, 6.22 and 6.28 in tap water, pond water and chlorinated water, respectively). After two weeks the pH started to increase again, and the increase further continued at three-weeks post mortem, where all the pHs increased to a value of around pH 7.0, with the smallest one remaining the saltwater one (pH 6.96).

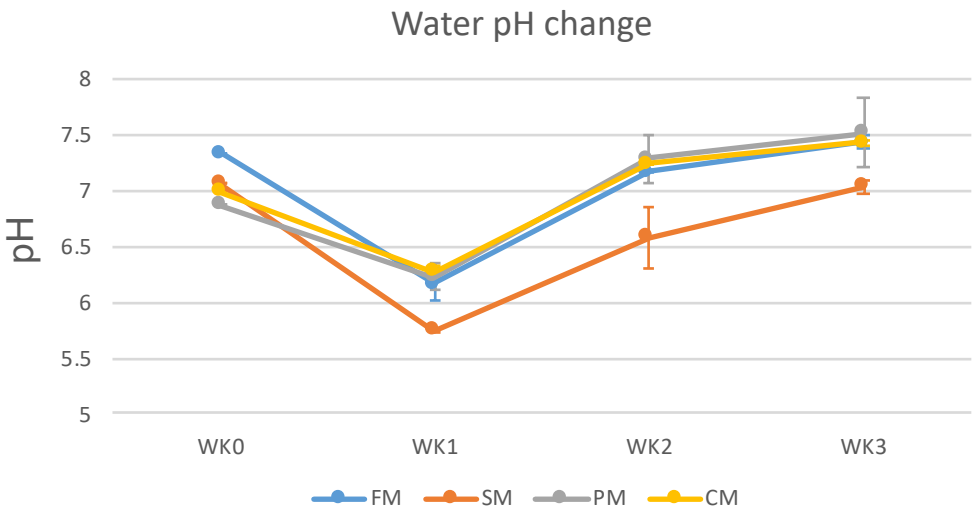

Fig. 1. A line graph illustrating the pH change at zero, one, two and three-week PMSI. (FM = tap water, SM = saltwater, PM = pond water, CM = chlorinated water) (WK0 = Zero-week PMSI, WK1 = One-week PMSI, WK2 = Two-weeks PMSI, WK3 = Three-weeks PMSI). The error bar of each line indicates the SE value of two replicates.

The greatest change in pH from time zero to one-week post mortem was measured in saltwater (ΔpH ≈ 1.3). The unexpected reduction of pH observed at week-one in this experiment could have been caused by the combination of post-mortem metabolism (e.g., glycolysis) in skeletal muscle and water buffering. It is widely accepted in the field of meat science that the pH value of mammalian skeletal muscles declines during the early post-mortem period due to glycolysis[56-59]. McGeehin *et al.*[57] similarly found that the pH of a lamb muscle decreased from 6.8 to 5.5 after 0.5, 1.5, 4 and 24 hours post mortem. However, it has been shown that the pH of terrestrial environments where a decomposing animal tissue is present increases, in contrast with the muscle itself. Carter and Tibbett[60] buried skeletal muscle of a lamb in soil and found a pH increase in grave soil after 7 days post mortem, followed by a constant decrease for the following 42 days. Similar findings are shown in Procopio *et al.*[61], where the grave soil pH started to increase after one-month PMI and increased further after two-months, subsequently decreasing from four months PMI onwards.

In both studies, the increase was explained as related to the increasing concentration of ammonium and nitrate in the grave soil. In aquatic environments, water acts as a buffer between intracellular and extracellular water, thereby allowing them to reach equilibrium, changing the chemical concentration and pH[62]. The decrease of water pH observed at one-week post mortem can be attributed to the an equilibrium induced by the buffer action of water or to an accumulation of ammonium – as suggested by Carter and Tibbett[60].

Proteomic results

A total of 41,003 MS/MS spectra were acquired by LC-MS/MS analyses and searched against Swiss-Prot with Mascot to perform identification. After the refinement steps previously mentioned, 2,789 different ions were matched. Where grouping samples were grouped according to their PMSI and on the basis of the relative abundance of proteins identified in each sample, 112 proteins showed an ANOVA *p* value smaller than 0.01 (and resulting *q* value smaller than 0.003), indicating a significant difference in their abundance between different PMSIs. When the samples were grouped according to the type of water used, we just found one protein with a *q* value smaller than 0.05, indicating a minor difference in protein abundances in relation to the type of water used for the experiment.

Proteomic differences according to different PMSIs

Protein relative abundances were calculated using Progenesis, and samples were grouped according to their PMSIs. Protein exports with normalized relative abundances were then used to plot PCAs using unique proteins whose relative abundances were significantly different across different PMSIs (N=112, Supporting Fig. S-1).

In order to highlight the most significant contributors to the clusters, the top 30 proteins ordered by their *q* value were selected for a second PCA plot (Fig. 2A). After this enrichment, the *q* value of the resulting candidates was smaller than 2.00e-4 (Table 2). Within the selected 30 proteins, nine of them were found more abundant in the controls, two of them after one-week and 18 of them after three-weeks post mortem. Samples with the same PMSI clustered together in the PCA, with the explained variance being of 52.5% for the first dimension (Dim1) and 21.3% for the second dimension (Dim2), respectively. Each cluster (time zero, one-week and three-weeks PMSI) was well-separated along both dimensions. The control cluster was separated from the other two along the second dimension predominantly, whereas the one-

and three-week clusters were separated mostly along the first dimension, showing a clear distinction between the two PMSIs overall. In short, bone proteomes of cadavers that were submerged in several water environments were modified differently according to their PMSIs. This result highlights the fact that proteomic investigations for PMSI estimation may be promising and should be pursued in the future. Results were also consistent with previous studies conducted on buried pig cadavers[51] and archaeological skeletal remains of humans[63], where the proteome was shown to be correlated with the PMI. It has to be pointed out that some of the biological replicates were found to be distinctly separated in the PCA (e.g., samples here named PM3_1 and PM3_2) due to potential intrinsic inter-individual differences. However, the results are consistent with the clustering obtained between the two different PMSIs.

The variable correlation plot (Fig. 2B and Table 2) showed that the control samples (PMSI = 0) were characterized by a higher relative abundance of ubiquitous proteins (e.g., proteins present in each cell despite the cell type, such as mitochondrial and ribosomal proteins), than the samples subjected to prolonged submersion. On the other hand, the one-week cluster was characterized by a higher relative abundance of bone-specific and serum proteins.

The results obtained here indicate that the type of proteins that are preferentially extracted from fresh bones are the ubiquitous ones, which leach from the body into the water within the first few days of decomposition not absorbed by hydroxyapatite. After the release of the ubiquitous and water-soluble proteins into the aquatic environment, the muscle tissue still partially present around the bones explains the higher relative abundance of muscle proteins found for the one-week PMSI samples. Finally, at three-weeks PMSI the decomposition stage of the muscles is more advanced, causing protein decay and a reduction in relative abundance of proteins in these samples.

At the same time, bone and blood proteins absorbed by hydroxyapatite were extracted from bones in a more efficient way than the other samples, due to deterioration of the bone structure exacerbated when bones is in contact with water, even when the flow of water is null (as in this case)[64]. In particular, several phenomena such as the dissolution of the mineral matrix and the enlargement of the pores of the bone structure can explain the increased release of acid-insoluble proteins during the extraction procedure[64].

Table 2. The top 30 proteins ordered by ANOVA *p* value when samples were grouped together according to their PMSIs. Group separations (A to E) have been further explained in Table 3.

Protein	Description	contributed to:	Category	ANOVA *p* value	q value
Group A (N=12)					
Col11a1	Collagen alpha-1(XI) chain	3 weeks	C	2.53E-05	6.71E-05
Col11a2	Collagen alpha-2(XI) chain	3 weeks	C	2.11E-05	6.71E-05
Hspg2	Basement membrane-specific heparan sulfate proteoglycan core protein	3 weeks	N	8.15E-06	4.45E-05
Alb	Serum albumin	3 weeks	B	2.43E-05	6.71E-05
Serpina3k	Serine protease inhibitor A3K	3 weeks	B	1.40E-05	5.26E-05
Apoa4	Apolipoprotein A-IV	3 weeks	B	3.69E-06	4.45E-05
Clec11a	C-type lectin domain family 11 member A	3 weeks	B	8.35E-05	1.36E-04
Nucb2	Necleobindin-2	3 weeks	U	9.41E-05	1.36E-04
App	Amyloid-beta A4 protein	3 weeks	U	8.85E-05	1.36E-04
Tpi1	Triosephosphate isomerase	1 week	U	3.75E-05	8.24E-05
Nme2	Nucleoside diphosphate kinase B	3 weeks	U	1.06E-05	4.45E-05
Serpinf1	Pigment epithelium-derived factor	3 weeks	U	6.32E-06	4.45E-05
Group B (N=6)					
Aldoa	Fructose-bisphophate aldolase A	0 week	M	4.92E-05	1.03E-04
Ppia	Peptidyl-prolyl cis-trans isomerase A	0 week	U	1.01E-05	4.45E-05
Rpl28	60S ribosomal protein L28	0 week	U	7.81E-06	4.45E-05
Hnrnpk	Heterogeneous nuclear ribonucleoprotein K	0 week	U	1.04E-05	4.45E-05
Aco2	Aconitate hydratase, mitochondrial	0 week	U	8.03E-05	1.36E-04
Tkt	Transketolase	0 week	U	3.02E-07	1.53E-05
Group C (N=3)					
Col1a2	Collagen alpha-2(I) chain	3 weeks	C	2.20E-05	6.71E-05
Lox	Protein-lysine 6-oxidase	3 weeks	C	6.93E-06	4.45E-05
Krt14	Keratin, type I cytoskeletal 14	3 weeks	U	3.21E-05	7.73E-05
Group D (N=2)					
Myh1	Myosin-1	1 week	M	3.37E-05	7.75E-05
Myh4	Myosin-4	1 week	M	3.76E-06	4.45E-05
Group E (N=7)					
Col3a1	Collagen alpha-1(III) chain	3 weeks	C	6.74E-05	1.22E-04
Col5a1	Collagen alpha-1(V) chain	3 weeks	C	9.51E-05	1.36E-04
Col1a1	Collagen alpha-1(I) chain	3 weeks	C	2.65E-05	6.71E-05
Tf	Serotransferrin	0 week	B	8.51E-05	1.36E-04

Myl1	Myosin light chain 1/3, skeletal muscle isoform	-	M	6.71E-05	1.22E-04
Pgk1	Phosphoglycerate kinase 1	0 week	U	5.11E-05	1.03E-04
Krt5	Keratin, type II cytoskeletal 5	3 weeks	U	1.46E-05	5.26E-05
C : Collagenous protein, N : NCP, B : Blood protein, M : Muscle protein, U : Ubiquitous protein 0 week : 0 week PMSI, 1 week : 1 week PMSI, 3 weeks : 3 weeks PMSI					

Table 3. Protein groups (columns, A to E) created to manually separate proteins depending on their abundance trends observed at specific PMSIs (one- and three-weeks PMSI).

	1 week	3 weeks
A	↓	↑
B	↓	↓
C	↑	↑
D	↑	↓
E	random	random

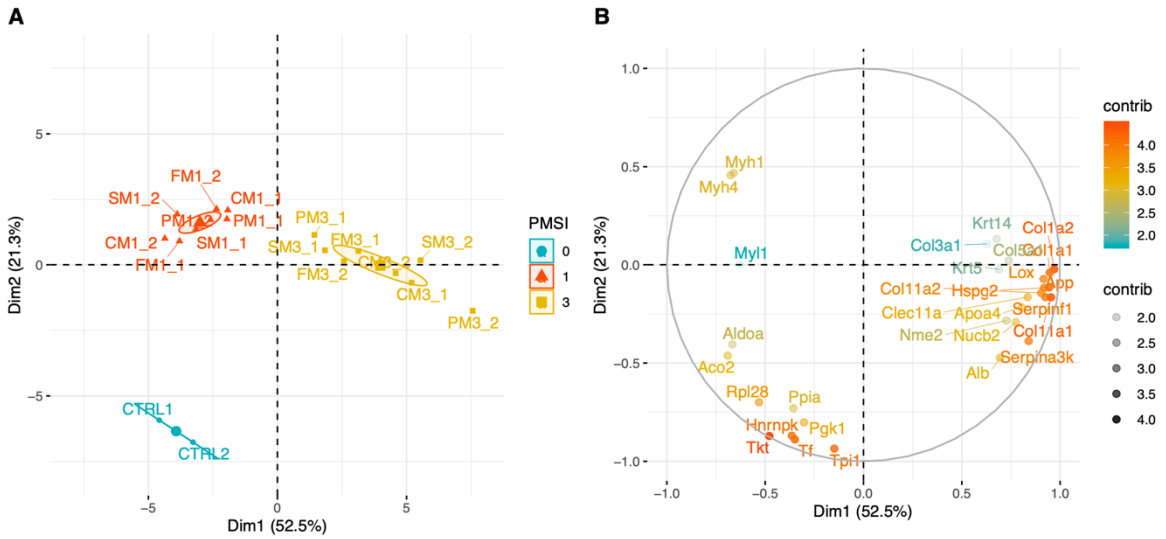

Fig. 2. (A) A Graph of PCA plot for different PMSIs calculated on top 30 proteins with the smallest *q* value. (CTRL = control samples, FM = tap water, SM = saltwater, PM = pond water, CM = chlorinated water). In each cluster, a bigger coordinate with the same colour was calculated as the mean coordinates, 'centroids', of the samples in the group. The same coloured icons indicate the same PMSI. The ellipse shows a cluster categorised by the same PMSI (confidence interval of 0.95) (PMSI 0 =zero-week PMSI, 1 = one-week PMSI, 3 = three-weeks PMSI) and centred on the centroid. **(B)** A variable correlation plot showing proteins that contributed to a cluster in the same direction on **A**. Proteins in red contributed more than the blue ones.

The top 30 proteins used in the PCA were manually divided into five groups according to their trends for the different PMSIs (e.g., if some proteins were constantly increasing or decreasing in abundance at a specific PMSI, they were grouped together) (Table 2 and 3, Fig. 3, Supporting Fig. S-2). Proteins in the first group (A) showed a decrease in their relative abundance at one-week PMSI, but an increase at three-weeks PMSI (N = 12). Proteins in the second group (B) showed a constant decrease in their relative abundance with increasing

PMSIs (N = 6). Proteins in the third group (C) showed an increased abundance steadily across all PMSIs (N = 3). The proteins whose abundance increased at one-week PMSI and decreased at three-weeks PMSI were classified into a fourth group (D, N = 2). In a final group (E), the proteins were those showing random trends according to different types of water (N = 7). Since one of the aims of the work was to identify useful biomarkers for PMSI estimation, we further focused on group B only.

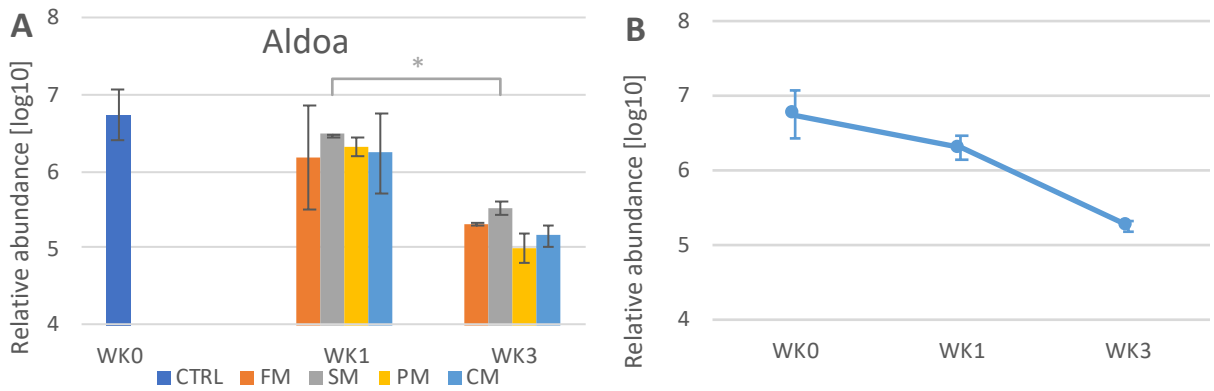

Fig. 3. (A) A bar graph of relative abundance of Aldoa. The same coloured lines indicate the same type of water (FM = tap water, SM = saltwater, PM = pond water, CM = chlorinated water). Each error bar is standard error (SE) calculated based on the relative abundances of two replicates in each condition. '*' means Student's t-Test *p* value was smaller than 0.05 between one-week and three-weeks PMSI in saltwater. **(B)** A line graph of averaged abundance of Aldoa at each PMSI for the two controls (WK0) and for all types of water (WK1 and WK3). (WK0 = Zero-week PMSI, WK1 = One-week PMSI, WK3 = Three-weeks PMSI).

With regard to the patterns observed in group B, (e.g., constant decrease of protein abundance with increasing PMSIs), it could be argued that these were due to constant degradation of proteins over the course of time and/or by constant leaching from the body in a time-related manner. Among the six proteins found in group B, all of them were ubiquitous proteins apart from Aldoa (Fig. 3A and B), one of the enzymes involved in glycolysis, that is specifically expressed in skeletal muscle (I band or M line)[65]. We believe that this protein may be a useful biomarker for PMSI estimation from bone (due to the proximity of bones and skeletal muscles *in vivo* that explains the recovery of muscle proteins from bones), and that further studies should be conducted on human remains and for prolonged periods of time in order to clarify for how long this protein can still be recovered in submerged bodies.

Several studies have demonstrated that post-mortem degradation of skeletal muscle and relevant proteins on exposed corpses occurs between 24 hours and 7 days PMI, just after the decomposition of other organs (e.g., kidney, liver and heart)[66, 67]. The degradation pattern of

Aldoa observed in this study indicates that the degradation of skeletal muscle in water started straight after the submersion of the remains, and continued for at least for three-weeks, consistent with the fact that the rate of decomposition in water is approximately half of the one calculated for bodies exposed to the air[68]. The results found here are also in agreement with what was found by Procopio *et al.*[51] for buried pigs, where a decrease in the abundance of Aldoa has been observed for the first two months post mortem, after which its abundance remained constant until the end of the experiment (six months PMI).

Additionally, we here evaluated the effects of increasing PMSIs on levels of fetuin-A (Fig. 4). Procopio *et al.*[51, 52] previously showed that the levels of fetuin-A are similar across different PMIs in terrestrial decomposition when the chronological age of the samples were similar. Furthermore, Procopio *et al.*[52] and Sawafuji *et al*.[63] showed that the normalized abundance of fetuin-A decreases with increasing biological age, and proposed its use as a biomarker to estimate the age of skeletal remains. Despite the similar biological age of all the mice used in this study, the relative abundance of fetuin-A was significantly different across increasing PMSIs (*q* value = 5.67e-4), decreasing from zero to one-week and increasing at three-weeks post mortem, thus sharing a similar trend in proteins previously grouped in group 'A', including albumin. This clearly differs from what has been found in terrestrial environments and could be due to exacerbated bone diagenesis in aquatic environments, as explained previously. Fetuin-A is a plasma protein produced by osteocytes[69, 70] and has been found to be preserved in archaeological samples[46, 63] without being affected by chronological age, making it a good potential target for biological age estimations.

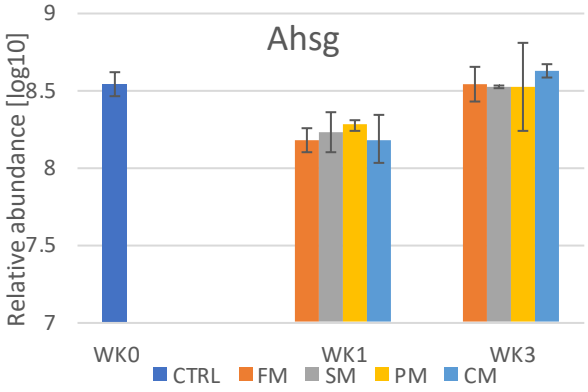

Fig. 4. A bar graph of relative abundance of fetuin-A (Ahsg). The same coloured lines indicate the same type of water (FM = tap water, SM = saltwater, PM = pond water, CM = chlorinated water). Each error bar is standard error (SE) calculated based on the relative abundances of two replicates in each condition. (WK0 = Zero-week PMSI, WK1 = One-week PMSI, WK3 = Three-weeks PMSI).

We believe that fetuin-A and albumin may have been resulted in being more abundant in the control samples due to the presence of peripheral blood that is, on the contrary, diluted in water in the submerged samples. Fetuin-A and albumin, in fact, can be both recovered from the peripheral blood and from the mineral matrix of the bone. Their strong interaction with the inorganic phase indicates they may be extracted more efficiently after prolonged times of submersion in water (three-week PMSI) than after shorter times (one-week PMSI), due to the presence of diagenetic phenomena which are normally affecting also the terrestrial environments. We hypothesize that this ultimately have led to an increased abundance of these two proteins at prolonged PMSIs, despite the fact this has not been reported previously for buried bodies[51]. For this reason, the potential usefulness of fetuin-A as a biomarker for biological age identification might be limited to cases of submerged remains.

Proteomic differences according to different types of water

It has been previously demonstrated that different types of water can alter the rate of body decomposition[71]. In order to test if the bone proteome of submerged bodies was affected by the presence of different types of water, we evaluated if proteins had significantly different abundances between control samples (time zero) and submerged samples in various types of water. Results showed that only one protein, namely peptidyl-prolyl cis-trans isomerase (PPIA), was significantly more abundant in the controls than in the water environments *(q* value = 0.037, Fig. 5), but we could not find other significant differences between the various water environments (Supporting Fig. S-3), as also showed by the PCA plot calculated with the top 30 proteins arranged by their *q* values (Supporting Fig. S-4) whose variance was explained for 57.8% along the first dimension and 12.4% along the second dimension. The control samples clustered far away from the submerged samples along the first dimension, whereas the four clusters of the submerged samples (tap water, saltwater, pond water and chlorinated water) were only partially separated along the second dimension, indicating that the bone proteome of the non-submerged bodies was significantly different compared to submerged ones. In order to improve the separation of the clusters we excluded the control samples from a newly calculated PCA whose explained variances were 37.2% in the first dimension and 15.7% in the second dimension (Fig. 6). In particular, the samples submerged in tap water (FM), pond water (PM) and chlorinated water (CM) clustered closely

each other, whereas the saltwater (SM) cluster was far apart from the others in the second dimension. The 3D PCA plot (Supporting Fig. S-5) further confirmed a clear separation of the SM cluster, also in the third dimension, which accounted for the 9.9% of the overall variation. Since the total explained variance of the bi-dimensional PCA (Fig. 6A) was less than 50% overall, it can be argued that the type of water only explained less than a half of the diversity observed in this study, and that most of the diversity was due to the previously mentioned PMSIs.

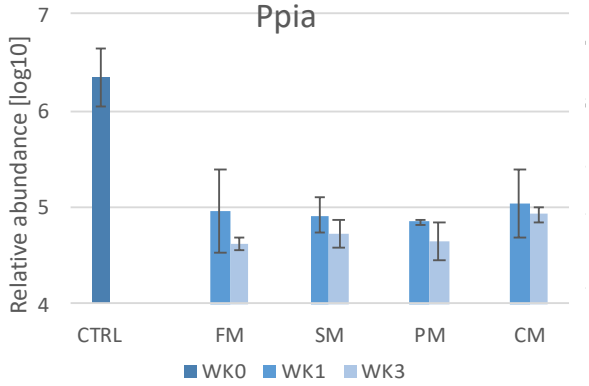

Fig. 5. Bar chart of relative abundance of Ppia. Dark blue indicates the relative abundance in the controls ('WK0'), blue indicates the relative abundance at one-week PMSI ('WK1') and light blue indicates that at three-weeks PMSI ('WK3'). Each error bar is standard error (SE) calculated based on the relative abundances of two replicates in each condition. (CTRL = control samples, FM = tap water, SM = saltwater, PM = pond water, CM = chlorinated water).

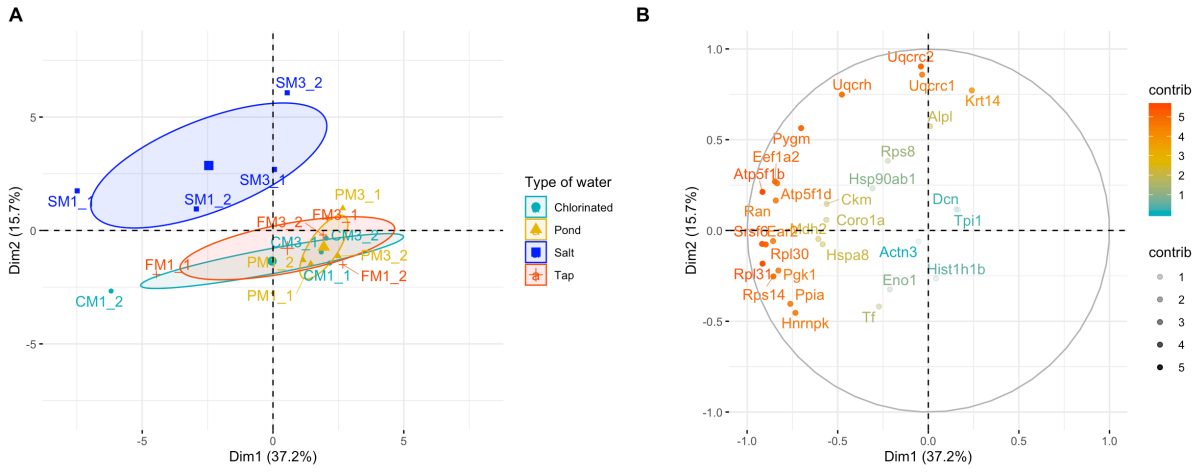

Fig. 6. (A) A graph of PCA plot with quantitative proteomic data without two control samples (CTRL1 and CTRL2) for different types of water calculated on top 30 proteins ordered according to their ANOVA *q* value. In each cluster, a bigger coordinate with the same colour was calculated as the mean coordinates, 'centroids', of the samples in the group. The ellipse shows a cluster categorised by the same type of water (confidence interval of 0.95) (FM = tap water, SM = saltwater, PM = pond water, CM = chlorinated water). **(B)** A variable correlation plot showing proteins that contributed to a cluster in the same location in **A**. A protein with a red plot indicates that it contributes more than that with a blue plot.

PPIA is an extracellular/secreted ubiquitous protein whose function is the acceleration of other protein's folding[72]. Despite it has never been reported previously in studies involving the cadaveric decomposition, its quick degradation in the aquatic environment may suggest that it could be a useful biomarker to indicate the submersion of a body, and could become a good target for additional studies in this field.

The effects of different PMSIs and types of water on protein deamidation

Among the list of peptides identified through the Mascot search, 79 had both a deamidated and a non-deamidated form. The focus of this study was on the NCPs specifically associated with bone tissue, muscle or blood, to find potential biomarkers for either PMSI estimation or indicators for the type of water in which bodies were submerged. For this reason, 35 out of 79 peptides that were matched to either collagenous or ubiquitous proteins were excluded from further analyses (Step 1 in Fig. 7). Deamidation ratios were calculated as previously described, and pairwise Student's t-Tests allowed the selection of a total of 19 significant peptides (Step 2 in Fig. 7). Peptides with a significantly different deamidation ratio within the same type of water or within the same PMSI were further selected (Step 3 in Fig. 7) and, as a result, nine peptides (assigned to four different proteins) were finally selected (Supporting Fig. S-6 as an example of tandem mass spectrum of non-deamidated and deamidated Ahsg peptide 'CNLLAEKQHGFCK'). We also evaluated the presence of peptides that were not deamidated in the controls, but were in the submerged samples (Step 4 in Fig. 7), and for this reason we added one further peptide to the list of selected peptides. Overall, we analyzed over all 10 peptides that matched six proteins (Table 4).

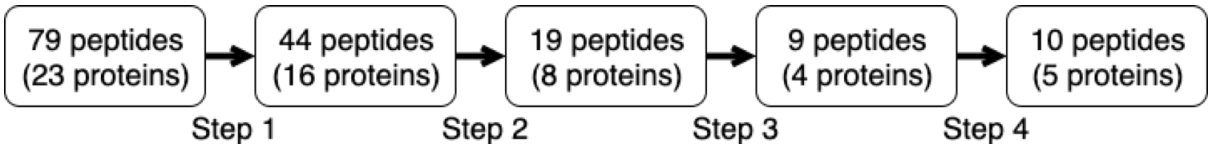

Fig. 7. The scheme used for peptide selection for deamidation ratio analysis. These steps were previously described in the methods section. In each step we showed the number of peptides and relative matched through Mascot.

Table 4. The list of 10 peptides selected for deamidation ratio analysis.

Protein	Category	Sequence	Significantly different between:	Highest deamidation ratio:	Student's t-Test *p* value
Within the same type of water (N=2)					
Ahsg	B	QVLNQIDKVK	SM1 - SM3	Three-weeks PMSI	1.15E-02
Igfbp5	B	CLPRQDEEKPLHALLHGR	CM1 - CM3		1.96E-02
Within the same PMSI (N=7)					
Ahsg	B	VGQPGAAGPVSPMCPGR	CM3 - SM3	Chlorinated	3.58E-02
		CNLLAEKQHGFCK	PM3 - SM3	Pond	1.81E-02
			CM3 - PM3		8.74E-03
		QVLNQIDKVK	CM1 - SM1	Chlorinated	1.28E-02
Apoe	B	TNLGAGAAQPLRDR	PM3 - FM3	Pond	1.67E-02
		LGQYRNEVHTMLGQSTEEIR	SM3 - FM3	Pond	2.03E-02
		GRLEEVGNQAR	CM1 - PM1	Pond	4.28E-02
Myh4	M	ESYVKATVQSR	CM3 - PM3	Chlorinated	1.11E-02
Other (N=1)					
F7	B	GKINHDIALLR	FM1 - CTRL	-	3.39E-03

Deamidated residue of asparagine (N) or glutamine (Q) was highlighted in red.
B : Blood protein, M : Muscle protein

Two of the 10 peptides selected for the deamidation study showed a significantly different deamidation ratio upon different PMSIs (Table 4). The peptide 'QVLNQIDKVK', with a deamidated Q in position 5, matched the protein fetuin-A (Ahsg) and was found to be more deamidated after three-weeks PMSI than after one week in saltwater, whereas the peptide 'CLPRQDEEKPLHALLHGR', with a deamidated Q in position 5, matched the insulin-like growth factor-binding protein (Igfbp5) and was found more deamidated after three-weeks PMSI than after one week in chlorinated water (Fig. 8).

Generally, the deamidation process of glutamine is well known to continue both *in vivo* with ageing phenomena and post mortem[73]. During terrestrial decomposition, it has been found that the deamidation of biglycan in bones increases with prolonged PMIs in a time-dependent way[51]. We confirmed in this study that the same phenomena took place in bodies decomposing in an aquatic environment and that, for those two proteins, the deamidation ratio increases from one to three-weeks PMSI.

Among the seven peptides that showed a Student's t-Test p value < 0.05 between different types of water at the same PMSI, a total of four peptides matching, respectively, fetuin-A (Ahsg, one peptide) and Apolipoprotein E (Apoe, three peptides), showed a higher

deamidation ratio in pond water compared with the other types of water (Fig. 8 and Supporting Fig. S-6). The other three peptides (two matching Ahsg and one matching Myh4), showed higher deamidation ratios in chlorinated water (Supporting Fig S-7). Previously, Pace *et al.*[74] showed that the asparagine deamidation rate of monoclonal antibodies is highly sensitive to extrinsic variables such as pH, type of buffer solution and temperature. They used different types of buffer and measured a slower deamidation ratio for antibodies suspended in histidine chloride and a faster deamidation ratio for antibodies in sodium phosphate (both at 40 °C). Capasso *et al.*[75] also showed that the deamidation mechanism of asparagine depends on the protein sequence, the pH and concentration of buffer solution, and the three-dimensional structure of the protein. Regarding glutamine deamidation, Liu *et al*.[76] also found that the deamidation ratio of glutamine was dependent on the pH of the solution. According to these studies and to our findings, it can be argued that a specific peptide would be deamidated in a different way in different aquatic environments depending on the previously cited extrinsic and intrinsic factors. This may also explain the differential deamidation ratios of different peptides of the same protein found in this study, as shown for the two peptides of Ahsg, and the cause could be due to different peptide sequences and their different position in the three-dimensional structure of the protein.

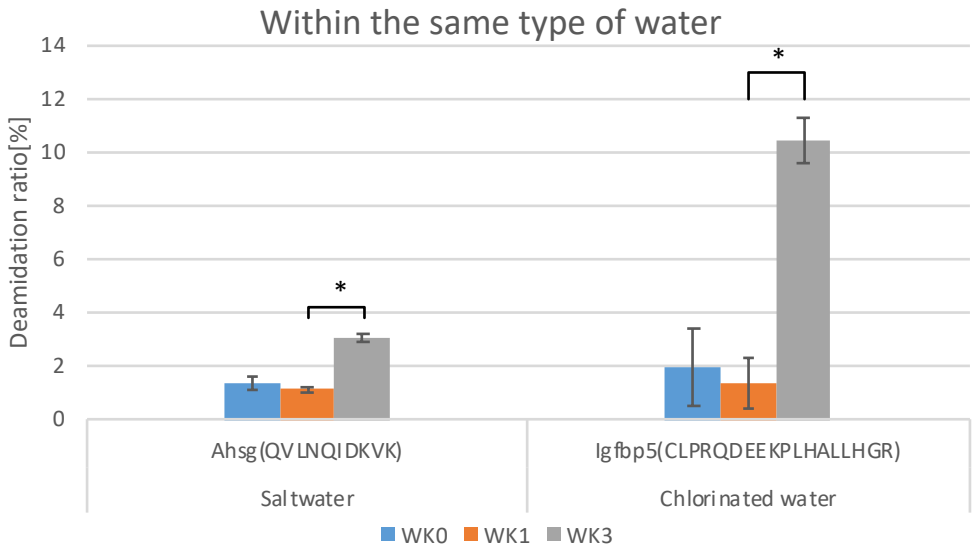

Fig. 8. Bar graphs of deamidation ratio of (left) the Ahsg peptide ('QVLNQIDKVK') in saltwater and (right) the Igfbp5 peptide ('CLPRQDEEKPLHALLHGR') in chlorinated water (WK0 = time zero PMSI, WK1 = one-week PMSI, WK3 = three-weeks PMSI). Error bar indicates SE value in each condition. '* 'shows a statistical significance for Student's t-Test (*p* value < 0.05) (see Table 4).

The higher deamidation ratios observed for pond water in comparison with the other types of water (Fig. 9) might be due to the presence of specific microorganisms and bacteria in pond water, which are missing in saltwater and in chlorinated water. Although deamidation of glutamine and asparagine was normally considered to be a non-enzymatic PTM[77], some studies have found that several enzymes, such as glutaminase or asparaginase, cause the deamidation[78, 79]. Glutaminase and asparaginase have been extracted from specific bacteria, such as *Bacillus circulans*[78], *Chryseobacterium proteolyticum*[77, 80] and *Trichosporon asahii*[81], and it has been verified that they are able to catalyze the deamidation of glutamine and asparagine residues. While the identification of the bacterial community present in the pond water used in this experiment was beyond the scope of this specific work, it can be argued that some bacteria present in pond water may have contributed to the increased deamidation levels due to their protein-glutaminase or asparaginase activities. However, pond water ecosystems (i.e., microbial and aquatic animal diversity) vary greatly from place to place, and may affect the deamidation of specific peptides in different ways. Therefore, the practical application of these peptides as a means to confirm the submersion of the body in a pond is very limited at this stage, and more tests using different types of pond water should be performed in order to better clarify the effects of the pond bacteria on the deamidation of the bone proteins.

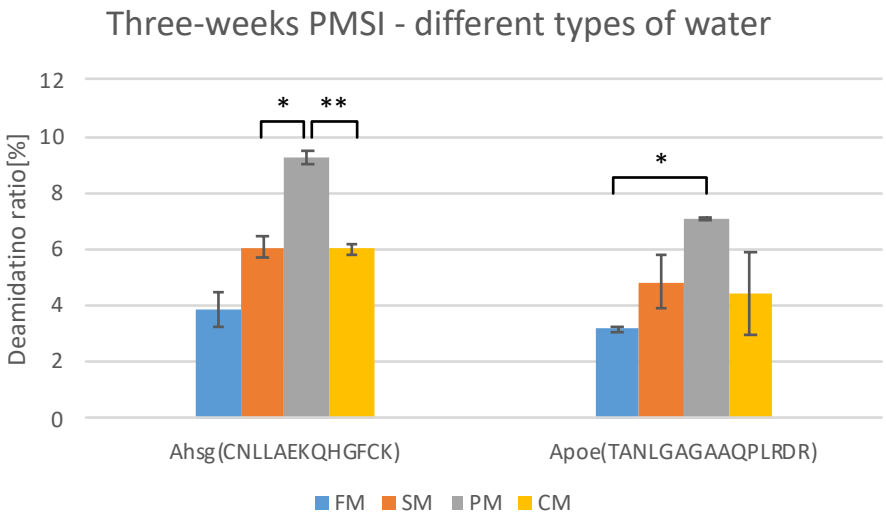

Fig. 9. Bar graphs of deamidation ratios of (left) the Ahsg peptide ('CNLLAEKQHGFCK') and (right) the Apoe peptide ('TANLGAGAAQPLRDR') at three-weeks PMSI (FM = tap water, SM = saltwater, PM = pond water, CM = chlorinated water). Error bar indicates SE value in each condition. '*' and '**' show a statistical significance for Student's t-Test (p value <0.05 and 0.01, respectively) (see Table 4).

In relation to the coagulation factor VII[82] (F7, peptide 'GKINHDIALLR', with a deamidated N in position 4), we found a significantly increased deamidation ratio between control samples at time zero and the samples submerged in tap water at one-week PMSI (Fig. 10, left). In particular, F7 was the only protein for which there were no deamidated peptides in both the control samples, but for which there were deamidated ones for the submerged samples. Due to the large SE values obtained from pond water and chlorinated water, we could not directly compare the deamidation levels for different types of water, and the deamidated ratios obtained for the two replicates were averaged in order to compare the results with the controls. To better clarify whether or not the deamidation observed for the submerged samples was specifically related to the submersion of the bodies or if it was also due to time-related post-mortem modifications, we evaluated the deamidation ratios of the six additional terrestrial controls. The averaged deamidated ratio using each set of six non-submerged samples (two controls at time zero, and four other controls decomposed for one and three weeks in a terrestrial environment) and submerged samples (FM1 x2 and FM3 x2) were calculated and compared (Fig. 10, right). We did not find any deamidation for this peptide in the terrestrial samples evaluated, therefore it could be concluded that the presence of the deamidated F7 forms might be specifically correlated with submersion in water, being a potential indicator of the submersion of a cadaver.

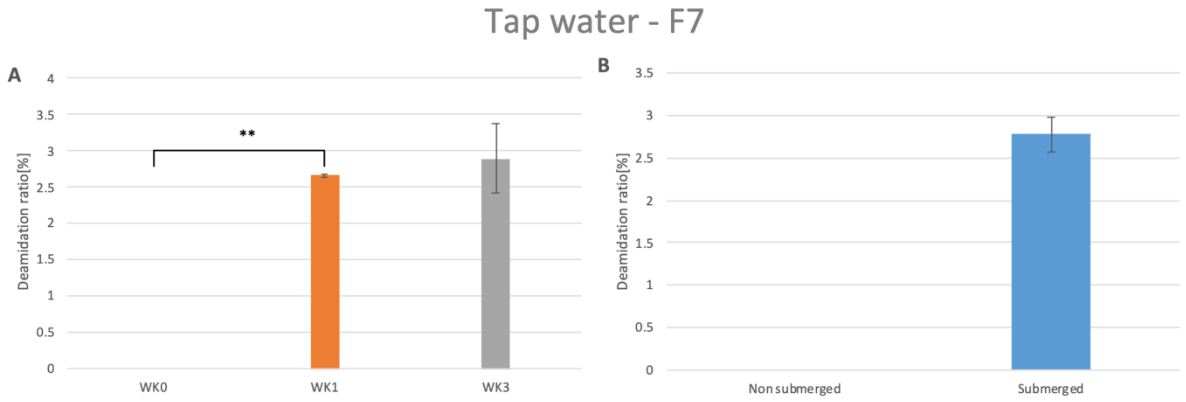

Fig. 10. Bar graphs of **(A)** deamidation ratio of F7 in tap water (WK0 = zero-week PMSI, WK1 = one-week PMSI, WK3 = three-weeks PMSI) and **(B)** averaged deamidation ratio of F7 using four samples both of non-submerged and submerged samples. In each graph, error bar indicates SE value in each condition. '**' means Student's t-Test *p* value is smaller than 0.01.

Conclusions

Overall, this study demonstrated the occurrence of specific bone proteome changes in submerged mouse cadavers that are different from the ones observed for buried or

exposed cadavers in terrestrial environments, and that PMSI is more able to affect the bone proteome recovery than the type of water used for the submersion. We found in particular that the muscle protein Aldoa could be used as potential biomarkers for PMSI estimation. We also showed that the reduced abundance of Ppia in bone samples, together with the presence of deamidations in protein F7 may be both useful to prove the submersion of a body in an aquatic environment. Moreover, we also showed here that the deamidation ratios of specific peptides could be useful for the estimation of PMSI and for the type of water. In particular, we showed that the deamidation ratio of two peptides matching fetuin-A and Igfbp5 significantly increased when PMSI increased, similar to what has been found previously for terrestrial environments for biglycan. Additionally, we showed that one peptide of fetuin-A was significantly more deamidated in pond water than in other types of water, revealing a potential new biomarker for the characterization of the type of water in which a cadaver has been submerged. Overall, the peptides identified may have the potential to become new biomarkers for the identification of specific post-mortem circumstances that could reveal new insights in investigations involving the presence of victims found in water or suspected of having decomposed in an aquatic environment. Further studies involving prolonged PMSI, human remains and the presence of the same types of water from different geographical locations will be required in order to allow the application of these findings to actual crime investigations, but the results proved the potential of the use of forensic proteomics to aquatic environments in order to reveal new information about the disposal of a victim that have never been obtained before.

The mass spectrometry proteomics data have been deposited to the ProteomeXchange Consortium via the PRIDE partner repository with the dataset identifier PXD017386 and 10.6019/PXD017386.

Supporting information

Table S-1. Measured pH values in water.

Fig. S-1. A PCA plot with 112 proteins that showed ANOVA *p* value < 0.01 and resulting *q* value < 0.003 when samples were grouped according to their PMSI.

Fig. S-2. Bar graphs of relative abundances changes of the top 30 proteins (ordered by their *q* value) used for PCA calculations when samples were grouped according to their PMSI.

Fig. S-3. Bar graphs of relative abundances changes of the top 30 proteins (ordered by their *q* value) used for PCA calculation when samples were grouped according to the different type of water.

Fig. S-4. 2D PCA plots using the top 30 proteins (ordered by their *q* value) whose relative abundances were different when grouping the samples according to the type of water.

Fig. S-5. 3D PCA plot using the top 30 proteins (ordered by their *q* value) whose relative abundances were different depending on the type of water.

Fig. S-6. Tandem mass spectra of non-deamidated and deamidated form of the Ahsg peptide.

Fig. S-7. Bar graphs showing deamidation ratios the peptides selected through the peptide selection for deamidation analysis (PDF).

Data S-1. Peptides and proteins list from Progenesis-exports: 'Peptide exports PMSI grouping', 'Protein exports PMSI grouping, 'Peptide exports type of water grouping' and 'Protein exports type of water grouping' (XLSX).

Acknowledgements

We acknowledge support from Northumbria University for funding this research. We also acknowledge the technical support from Dr. William Cheung at the NUOmics Facility, who conducted LC-MS/MS analysis and provided the raw data, and from Prof. Martin Evison, who proofread the manuscript.

References

1. Simmons, T., Post-Mortem Interval Estimation: an Overview of Techniques. In *Taphonomy of Human Remains: Forensic Analysis of the Dead and the Depositional Environment*, Schotsmans, E. M.; Márquez-Grant, N.; Forbes, S. L., Eds. Wiley: 2017; pp 134-142.
2. Ubelaker, D. H., Taphonomic Applications in Forensic Anthoropology. In *Forensic Taphonomy: The Postmortem Fate of Human Remains*, 1st ed.; Haglund, W. D.; Sorg, M. H., Eds. CRC Press: 1996; pp 77-90.
3. Goff, M., Early post-mortem changes and stages of decomposition in exposed cadavers. *Experimental and Applied Acarology* **2009,** *49* (1-2), 21-36.
4. Muggenthaler, H.; Sinicina, I.; Hubig, M.; Mall, G., Database of post-mortem rectal cooling cases under strictly controlled conditions: a useful tool in death time estimation. *International Journal of Legal Medicine* **2012,** *126* (1), 79-87.
5. Amendt, J.; Richards, C.; Campobasso, C.; Zehner, R.; Hall, M., Forensic entomology: applications and limitations. *Forensic Science Medicine and Pathology* **2011,** *7* (4), 379-392.
6. Vass, A. A., The elusive universal post-mortem interval formula. *Forensic Science International* **2011,** *204* (1-3), 34-40.
7. Cockle, D.; Bell, L., Human decomposition and the reliability of a 'Universal' model for post mortem interval estimations. *Forensic Science International* **2015,** *253*, 136.e1-136.e9.
8. Carter, D.; Yellowlees, D.; Tibbett, M., Cadaver decomposition in terrestrial ecosystems. *Naturwissenschaften* **2007,** *94* (1), 12-24.
9. Carter, D.; Yellowlees, D.; Tibbett, M., Temperature affects microbial decomposition of cadavers (Rattus rattus) in contrasting soils. *Applied Soil Ecology* **2008,** *40* (1), 129-137.
10. Ferreira, M.; Cunha, E., Can we infer post mortem interval on the basis of decomposition rate? A case from a Portuguese cemetery. *Forensic Science International* **2013,** *226* (1-3), 298.e1-298.e6.
11. Heaton, V.; Lagden, A.; Moffatt, C.; Simmons, T., Predicting the Postmortem Submersion Interval for Human Remains Recovered from UK Waterways. *Journal of Forensic Sciences* **2010,** *55* (2), 302-307.
12. Sorg, M. H.; Dearborn, J. H.; Monahan, E. I.; Ryan, H. F.; Sweeney, K. G.; David, E., Forensic Taphonomy in Marine Contexts. In *Forensic Taphonomy: The Postmortem Fate of Human Remains*, 1st ed.; Sorg, M. H.; Haglund, W. D., Eds. CRC Press: 1996; pp 567-604.
13. Dickson, G.; Poulter, R.; Maas, E.; Probert, P.; Kieser, J., Marine bacterial succession as a potential indicator of postmortem submersion interval. *Forensic Science International* **2011,** *209* (1-3), 1-10.
14. Reijnen, G.; Gelderman, H.; Grotebevelsborg, B.; Reijnders, U.; Duijst, W., The correlation between the Aquatic Decomposition Score (ADS) and the post-mortem submersion interval measured in Accumulated Degree Days (ADD) in bodies recovered from fresh water. *Forensic Science Medicine and Pathology* **2018,** *14* (3), 301-306.
15. van Daalen, M.; de Kat, D.; Grotebevelsborg, B.; de Leeuwe, R.; Warnaar, J.; Oostra, R.; Duijst-Heesters, W., An Aquatic Decomposition Scoring Method to Potentially Predict the Postmortem Submersion Interval of Bodies Recovered from the North Sea. *Journal of Forensic Sciences* **2017,** *62* (2), 369-373.
16. Humphreys, M. K.; Panacek, E.; Green, W.; Albers, E., Comparison of protocols for measuring and calculating postmortem submersion intervals for human analogs in fresh water. *J Forensic Sci* **2013,** *58* (2), 513-7.
17. De Donno, A.; Campobasso, C. P.; Santoro, V.; Leonardi, S.; Tafuri, S.; Introna, F., Bodies in sequestered and non-sequestered aquatic environments: a comparative taphonomic study using decompositional scoring system. *Sci Justice* **2014,** *54* (6), 439-46.
18. Ciaffi, R.; Feola, A.; Perfetti, E.; Manciocchi, S.; Potenza, S.; Marella, G., Overview on the estimation of post mortem interval in forensic anthropology: review of the literature and practical experience. *Romanian Journal of Legal Medicine* **2018,** *26* (4), 403-411.

19. Jopp-van Well, E.; Augustin, C.; Busse, B.; Fuhrmann, A.; Hahn, M.; Tsokos, M.; Verhoff, M.; Schulze, F., The assessment of adipocere to estimate the post-mortem interval - a skeleton from the tidelands. *Anthropologischer Anzeiger* **2016,** *73* (3), 235-247.
20. Widya, M.; Moffatt, C.; Simmons, T., The Formation of Early Stage Adipocere in Submerged Remains: A Preliminary Experimental Study*. *Journal of Forensic Sciences* **2012,** *57* (2), 328-333.
21. Grassberger, M.; Friedrich, E.; Reiter, C., The blowfly Chrysomya albiceps (Wiedemann) (Diptera : Calliphoridae) as a new forensic indicator in Central Europe. *International Journal of Legal Medicine* **2003,** *117* (2), 75-81.
22. Barrios, M.; Wolff, M., Initial study of arthropods succession and pig carrion decomposition in two freshwater ecosystems in the Colombian Andes. *Forensic Science International* **2011,** *212* (1-3), 164-172.
23. O'Brien, T. G.; Kuehner, A. C., Waxing grave about adipocere: soft tissue change in an aquatic context. *J Forensic Sci* **2007,** *52* (2), 294-301.
24. Forbes, S. L.; Wilson, M. E.; Stuart, B. H., Examination of adipocere formation in a cold water environment. *Int J Legal Med* **2011,** *125* (5), 643-50.
25. Dickson, G. C.; Poulter, R. T.; Maas, E. W.; Probert, P. K.; Kieser, J. A., Marine bacterial succession as a potential indicator of postmortem submersion interval. *Forensic Sci Int* **2011,** *209* (1-3), 1-10.
26. Kang, S.; Kassam, N.; Gauthier, M.; O'Day, D., Post-mortem changes in calmodulin binding proteins in muscle and lung. *Forensic Science International* **2003,** *131* (2-3), 140-147.
27. Kwak, J.; Kim, H.; Kim, K.; Noh, B.; Cheon, H.; Yeo, M.; Shakya, R.; Shrestha, S.; Kim, D.; Choe, S.; Pyo, J., Proteomic Evaluation of Biomarkers to Determine the Postmortem Interval. *Analytical Letters* **2017,** *50* (1), 207-218.
28. Kumar, S.; Ali, W.; Singh, U.; Kumar, A.; Bhattacharya, S.; Verma, A., The effect of elapsed time on the cardiac Troponin-T (cTnT) proteolysis in case of death due to burn: A study to evaluate the potential forensic use of cTnT to determine the postmortem interval. *Science & Justice* **2015,** *55* (3), 189-194.
29. Kumar, S.; Ali, W.; Singh, U.; Kumar, A.; Bhattacharya, S.; Verma, A.; Rupani, R., Temperature-Dependent Postmortem Changes in Human Cardiac Troponin-T (cTnT): An Approach in Estimation of Time Since Death. *Journal of Forensic Sciences* **2016,** *61*, S241-S245.
30. Poloz, Y.; O'Day, D., Determining time of death: temperature-dependent postmortem changes in calcineurin A, MARCKS, CaMKII, and protein phosphatase 2A in mouse. *International Journal of Legal Medicine* **2009,** *123* (4), 305-314.
31. Choi, K.; Zissler, A.; Kim, E.; Ehrenfellner, B.; Cho, E.; Lee, S.; Steinbacher, P.; Yun, K.; Shin, J.; Kim, J.; Stoiber, W.; Chung, H.; Monticelli, F.; Pittner, S., Postmortem proteomics to discover biomarkers for forensic PMI estimation. *International Journal of Legal Medicine* **2019,** *133* (3), 899-908.
32. Sampaio-Silva, F.; Magalhaes, T.; Carvalho, F.; Dinis-Oliveira, R.; Silvestre, R., Profiling of RNA Degradation for Estimation of Post Morterm Interval. *Plos One* **2013,** *8* (2), e56507.
33. Tu, C.; Du, T.; Ye, X.; Shao, C.; Xie, J.; Shen, Y., Using miRNAs and circRNAs to estimate PMI in advanced stage. *Legal Medicine* **2019,** *38*, 51-57.
34. Ahmed, M.; Gardiner, K., Preserving protein profiles in tissue samples: Differing outcomes with and without heat stabilization. *Journal of Neuroscience Methods* **2011,** *196* (1), 99-106.
35. Merkley, E.; Wunschel, D.; Wahl, K.; Jarman, K., Applications and challenges of forensic proteomics. *Forensic Science International* **2019,** *297*, 350-363.
36. Kaiser, C.; Bachmeier, B.; Conrad, C.; Nerlich, A.; Bratzke, H.; Eisenmenger, W.; Peschel, O., Molecular study of time dependent changes in DNA stability in soil buried skeletal residues. *Forensic Science International* **2008,** *177* (1), 32-36.
37. Cook, G.; MacKenzie, A., Radioactive isotope analyses of skeletal materials in forensic science: a review of uses and potential uses. *International Journal of Legal Medicine* **2014,** *128* (4), 685-698.
38. Mello, R. B.; Silva, M. R.; Alves, M. T.; Evison, M. P.; Guimarães, M. A.; Francisco, R. A.; Astolphi, R. D.; Iwamura, E. S., Tissue Microarray Analysis Applied to Bone Diagenesis. *Sci Rep* **2017,** *7*, 39987.

39. Longato, S.; Woss, C.; Hatzer-Grubwieser, P.; Bauer, C.; Parson, W.; Unterberger, S.; Kuhn, V.; Pemberger, N.; Pallua, A.; Recheis, W.; Lackner, R.; Stalder, R.; Pallua, J., Post-mortem interval estimation of human skeletal remains by micro-computed tomography, mid-infrared microscopic imaging and energy dispersive X-ray mapping. *Analytical Methods* **2015,** *7* (7), 2917-2927.
40. Woess, C.; Unterberger, S.; Roider, C.; Ritsch-Marte, M.; Pemberger, N.; Cemper-Kiesslich, J.; Hatzer-Grubwieser, P.; Parson, W.; Pallua, J., Assessing various Infrared (IR) microscopic imaging techniques for post-mortem interval evaluation of human skeletal remains. *Plos One* **2017,** *12* (3), e0174552.
41. Buekenhout, I.; Vieira, D.; Ferreira, M., Reliability of weathering in the estimation of the post-mortem interval of human remains buried in coffins. *Australian Journal of Forensic Sciences* **2018,** *50* (4), 414-427.
42. Procopio, N.; Buckley, M., Minimizing Laboratory-Induced Decay in Bone Proteomics. *Journal of Proteome Research* **2017,** *16* (2), 447-458.
43. Collins, M. J.; Riley, M. S.; Child, A. M.; Turnerwalker, G., A Basic Mathematical Simulation of the Chemical Degradation of Ancient Collagen. *Journal of Archaeological Science* **1995,** *22* (2), 175-183.
44. Clarke, B., Normal Bone Anatomy and Physiology. *Clinical Journal of the American Society of Nephrology* **2008,** *3*, S131-S139.
45. Prieto-Bonete, G.; Perez-Carceles, M.; Maurandi-Lopez, A.; Perez-Martinez, C.; Luna, A., Association between protein profile and postmortem interval in human bone remains. *Journal of Proteomics* **2019,** *192*, 54-63.
46. Wadsworth, C.; Buckley, M., Proteome degradation in fossils: investigating the longevity of protein survival in ancient bone. *Rapid Commun Mass Spectrom* **2014,** *28* (6), 605-15.
47. Cappellini, E.; Jensen, L. J.; Szklarczyk, D.; Ginolhac, A.; da Fonseca, R. A.; Stafford, T. W.; Holen, S. R.; Collins, M. J.; Orlando, L.; Willerslev, E.; Gilbert, M. T.; Olsen, J. V., Proteomic analysis of a pleistocene mammoth femur reveals more than one hundred ancient bone proteins. *J Proteome Res* **2012,** *11* (2), 917-26.
48. Wadsworth, C.; Procopio, N.; Anderung, C.; Carretero, J. M.; Iriarte, E.; Valdiosera, C.; Elburg, R.; Penkman, K.; Buckley, M., Comparing ancient DNA survival and proteome content in 69 archaeological cattle tooth and bone samples from multiple European sites. *J Proteomics* **2017,** *158*, 1-8.
49. Boaks, A.; Siwek, D.; Mortazavi, F., The temporal degradation of bone collagen: A histochemical approach. *Forensic Science International* **2014,** *240*, 104-110.
50. Jellinghaus, K.; Hachmann, C.; Hoeland, K.; Bohnert, M.; Wittwer-Backofen, U., Collagen degradation as a possibility to determine the post-mortem interval (PMI) of animal bones: a validation study referring to an original study of Boaks et al. (2014). *International Journal of Legal Medicine* **2018,** *132* (3), 753-763.
51. Procopio, N.; Williams, A.; Chamberlain, A.; Buckley, M., Forensic proteomics for the evaluation of the post-mortem decay in bones. *Journal of Proteomics* **2018,** *177*, 21-30.
52. Procopio, N.; Chamberlain, A.; Buckley, M., Intra- and Interskeletal Proteome Variations in Fresh and Buried Bones. *Journal of Proteome Research* **2017,** *16* (5), 2016-2029.
53. Deininger, L.; Patel, E.; Clench, M. R.; Sears, V.; Sammon, C.; Francese, S., Proteomics goes forensic: Detection and mapping of blood signatures in fingermarks. *Proteomics* **2016,** *16* (11-12), 1707-17.
54. Oonk, S.; Schuurmans, T.; Pabst, M.; de Smet, L. C. P. M.; de Puit, M., Proteomics as a new tool to study fingermark ageing in forensics. *Sci Rep* **2018,** *8* (1), 16425.
55. Gundry, R. L.; White, M. Y.; Murray, C. I.; Kane, L. A.; Fu, Q.; Stanley, B. A.; Van Eyk, J. E., Preparation of proteins and peptides for mass spectrometry analysis in a bottom-up proteomics workflow. *Curr Protoc Mol Biol* **2009,** *Chapter 10*, Unit10.25.
56. Ferguson, D.; Gerrard, D., Regulation of post-mortem glycolysis in ruminant muscle. *Animal Production Science* **2014,** *54* (4), 464-481.
57. McGeehin, B.; Sheridan, J.; Butler, F., Factors affecting the pH decline in lamb after slaughter. *Meat Science* **2001,** *58* (1), 79-84.

58. D'Alessandro, A.; Zolla, L., Meat science: From proteomics to integrated omics towards system biology. *Journal of Proteomics* **2013,** *78*, 558-577.
59. Zhang, L.; Liu, R.; Cheng, Y.; Xing, L.; Zhou, G.; Zhang, W., Effects of protein S-nitrosylation on the glycogen metabolism in postmortem pork. *Food Chem* **2019,** *272*, 613-618.
60. Carter, D.; Tibbett, M., Does repeated burial of skeletal muscle tissue (Ovis aries) in soil affect subsequent decomposition? *Applied Soil Ecology* **2008,** *40* (3), 529-535.
61. Procopio, N.; Ghignone, S.; Williams, A.; Chamberlain, A.; Mello, A.; Buckley, M., Metabarcoding to investigate changes in soil microbial communities within forensic burial contexts. *Forensic Sci Int Genet* **2019,** *39*, 73-85.
62. Gill-King, H., Chemical and Ultrastructural Aspects of Decomposition. In *Forensic Taphonomy: The Postmortem Fate of Human Remains*, Sorg, M. H.; Haglund, W. D., Eds. CRC Press: Boca Raton, London, 1996; pp 93-108.
63. Sawafuji, R.; Cappellini, E.; Nagaoka, T.; Fotakis, A. K.; Jersie-Christensen, R. R.; Olsen, J. V.; Hirata, K.; Ueda, S., Proteomic profiling of archaeological human bone. *R Soc Open Sci* **2017,** *4* (6), 161004.
64. Hedges, R. E. M.; Millard, A. R., Bones and Groundwater: Towards the Modelling of Diagenetic Processes. *Journal of Archaeological Science* **1995,** *22* (2), 155-164.
65. Paolella, G.; Buono, P.; Mancini, F. P.; Izzo, P.; Salvatore, F., Structure and expression of mouse aldolase genes. Brain-specific aldolase C amino acid sequence is closely related to aldolase A. *Eur J Biochem* **1986,** *156* (2), 229-35.
66. Pittner, S.; Ehrenfellner, B.; Monticelli, F. C.; Zissler, A.; Sänger, A. M.; Stoiber, W.; Steinbacher, P., Postmortem muscle protein degradation in humans as a tool for PMI delimitation. *Int J Legal Med* **2016,** *130* (6), 1547-1555.
67. Pittner, S.; Monticelli, F. C.; Pfisterer, A.; Zissler, A.; Sanger, A. M.; Stoiber, W.; Steinbacher, P., Postmortem degradation of skeletal muscle proteins: a novel approach to determine the time since death. *International Journal of Legal Medicine* **2016,** *130* (2), 421-431.
68. Lawler, W., Bodies recovered from water: a personal approach and consideration of difficulties. *J Clin Pathol* **1992,** *45* (8), 654-9.
69. Szweras, M.; Liu, D. M.; Partridge, E. A.; Pawling, J.; Sukhu, B.; Clokie, C.; Jahnen-Dechent, W.; Tenenbaum, H. C.; Swallow, C. J.; Grynpas, M. D.; Dennis, J. W., alpha 2-HS glycoprotein/fetuin, a transforming growth factor-beta/bone morphogenetic protein antagonist, regulates postnatal bone growth and remodeling. *Journal of Biological Chemistry* **2002,** *277* (22), 19991-19997.
70. Mattinzoli, D.; Rastaldi, M. P.; Ikehata, M.; Armelloni, S.; Pignatari, C.; Giardino, L. A.; Li, M.; Alfieri, C. M.; Regalia, A.; Riccardi, D.; Messa, P., FGF23-regulated production of Fetuin-A (AHSG) in osteocytes. *Bone* **2016,** *83*, 35-47.
71. Stuart, B. H.; Ueland, M., Decomposition in Aquatic Environments. In *Taphonomy of Human Remains: Forensic Analysis of the Dead and the Depositional Environment*, E. M. Schotsmans; Márquez-Grant, N.; Forbes, S. L., Eds. Wiley: Chichester, England, 2017; pp 235 - 250.
72. Hillier, L. W.; Fulton, R. S.; Fulton, L. A.; Graves, T. A.; Pepin, K. H.; Wagner-McPherson, C.; Layman, D.; Maas, J.; Jaeger, S.; Walker, R.; Wylie, K.; Sekhon, M.; Becker, M. C.; O'Laughlin, M. D.; Schaller, M. E.; Fewell, G. A.; Delehaunty, K. D.; Miner, T. L.; Nash, W. E.; Cordes, M.; Du, H.; Sun, H.; Edwards, J.; Bradshaw-Cordum, H.; Ali, J.; Andrews, S.; Isak, A.; Vanbrunt, A.; Nguyen, C.; Du, F.; Lamar, B.; Courtney, L.; Kalicki, J.; Ozersky, P.; Bielicki, L.; Scott, K.; Holmes, A.; Harkins, R.; Harris, A.; Strong, C. M.; Hou, S.; Tomlinson, C.; Dauphin-Kohlberg, S.; Kozlowicz-Reilly, A.; Leonard, S.; Rohlfing, T.; Rock, S. M.; Tin-Wollam, A. M.; Abbott, A.; Minx, P.; Maupin, R.; Strowmatt, C.; Latreille, P.; Miller, N.; Johnson, D.; Murray, J.; Woessner, J. P.; Wendl, M. C.; Yang, S. P.; Schultz, B. R.; Wallis, J. W.; Spieth, J.; Bieri, T. A.; Nelson, J. O.; Berkowicz, N.; Wohldmann, P. E.; Cook, L. L.; Hickenbotham, M. T.; Eldred, J.; Williams, D.; Bedell, J. A.; Mardis, E. R.; Clifton, S. W.; Chissoe, S. L.; Marra, M. A.; Raymond, C.; Haugen, E.; Gillett, W.; Zhou, Y.; James, R.; Phelps, K.; Iadanoto, S.; Bubb, K.; Simms, E.; Levy, R.; Clendenning, J.; Kaul, R.; Kent, W. J.; Furey, T. S.; Baertsch, R. A.; Brent, M. R.; Keibler, E.; Flicek, P.; Bork, P.; Suyama, M.; Bailey, J. A.; Portnoy, M. E.; Torrents, D.; Chinwalla, A. T.; Gish, W. R.; Eddy, S. R.; McPherson, J. D.; Olson, M. V.; Eichler, E. E.; Green,

E. D.; Waterston, R. H.; Wilson, R. K., The DNA sequence of human chromosome 7. *Nature* **2003,** *424* (6945), 157-64.
73. van Doorn, N.; Wilson, J.; Hollund, H.; Soressi, M.; Collins, M., Site-specific deamidation of glutamine: a new marker of bone collagen deterioration. *Rapid Communications in Mass Spectrometry* **2012,** *26* (19), 2319-2327.
74. Pace, A. L.; Wong, R. L.; Zhang, Y. T.; Kao, Y. H.; Wang, Y. J., Asparagine deamidation dependence on buffer type, pH, and temperature. *J Pharm Sci* **2013,** *102* (6), 1712-1723.
75. Capasso, S.; Mazzarella, L.; Sica, F.; Zagari, A.; Salvadori, S., Kinetics and mechanism of succinimide ring formation in the deamidation process of asparagine residues. *Journal of the Chemical Society-Perkin Transactions 2* **1993,** (4), 679-682.
76. Liu, H.; Gaza-Bulseco, G.; Chumsae, C., Glutamine deamidation of a recombinant monoclonal antibody. *Rapid Commun Mass Spectrom* **2008,** *22* (24), 4081-8.
77. Yamaguchi, S.; Jeenes, D. J.; Archer, D. B., Protein-glutaminase from Chryseobacterium proteolyticum, an enzyme that deamidates glutaminyl residues in proteins. Purification, characterization and gene cloning. *Eur J Biochem* **2001,** *268* (5), 1410-21.
78. Kikuchi, M.; Hayashida, H.; Nakano, E.; Sakaguchi, K., Peptidoglutaminase. Enzymes for selective deamidation of gamma-amide of peptide-bound glutamine. *Biochemistry* **1971,** *10* (7), 1222-9.
79. Miwa, N.; Mitsuhashi, M.; Kajiura, T., Screening of microorganisms producing a novel protein-asparaginase and characterization of the enzyme derived from Luteimicrobium album. *J Biosci Bioeng* **2019,** *127* (3), 281-287.
80. Yamaguchi, S.; Yokoe, M., A novel protein-deamidating enzyme from Chryseobacterium proteolyticum sp. nov., a newly isolated bacterium from soil. *Appl Environ Microbiol* **2000,** *66* (8), 3337-43.
81. Ashok, A.; Doriya, K.; Rao, J. V.; Qureshi, A.; Tiwari, A. K.; Kumar, D. S., Microbes Producing L-Asparaginase free of Glutaminase and Urease isolated from Extreme Locations of Antarctic Soil and Moss. *Sci Rep* **2019,** *9* (1), 1423.
82. Pinotti, M.; Bertolucci, C.; Portaluppi, F.; Colognesi, I.; Frigato, E.; Foà, A.; Bernardi, F., Daily and circadian rhythms of tissue factor pathway inhibitor and factor VII activity. *Arterioscler Thromb Vasc Biol* **2005,** *25* (3), 646-9.

For TOC/Abstract Graphic only: